Published in final edited form as:

J Magn Reson Imaging. 2019 April ; 49(4): 994–1005. doi:10.1002/jmri.26305.

Hemodynamic measurements with an abdominal 4D flow MRI sequence with spiral sampling and compressed sensing in patients with chronic liver disease.

Octavia Bane, PhD[1,2], **Steven Peti, MD**[1], **Mathilde Wagner, MD, PhD**[2,3], **Stefanie Hectors, PhD**[1,2], **Hadrien Dyvorne, PhD**[2,4], **Michael Markl, PhD**[5,6], and **Bachir Taouli, MD**[1,2]

[1]Department of Radiology, Icahn School of Medicine at Mount Sinai, New York, NY

[2]Translational and Molecular Imaging Institute, Icahn School of Medicine at Mount Sinai, New York, NY

[3]Department of Radiology, Groupe Hospitalier Pitié Salpêtrière, Paris, France

[4]4Catalyzer, Guilford, CT

[5]Radiology, Northwestern University Feinberg School of Medicine, Chicago, IL

[6]Biomedical Engineering, Northwestern University, Evanston, IL

Abstract

BACKGROUND: The test-retest/interobserver repeatability and diagnostic value of 4D flow MRI in liver disease is under-reported.

PURPOSE: To determine the reproducibility/repeatability of flow quantification in abdominal vessels using a spiral 4D flow MRI sequence; to assess the value of 4D flow parameters in diagnosing cirrhosis and degree of portal hypertension.

STUDY TYPE: Prospective.

SUBJECTS: 52 patients with chronic liver disease.

FIELD STRENGTH/SEQUENCE: 1.5T/spiral 4D flow acquired in 1 breath-hold.

ASSESSMENT: Thirteen abdominal vessels were identified and segmented by 2 independent observers to measure maximum and time-averaged through-plane velocity, net flow and vessel cross-section area. Interobserver agreement and test-retest repeatability were evaluated in 15 and 4 cases, respectively. Prediction of the presence and severity of cirrhosis and portal hypertension was assessed using 4D flow parameters.

STATISTICAL TESTS: Cohen's kappa coefficient, coefficient of variation (CV), Bland-Altman, Mann-Whitney tests, logistic regression.

Results: For all vessels combined, measurements showed acceptable agreement between observers, with Cohen's kappa=0.70($p<0.001$), CV<21%, Bland-Altman bias <5%, but high limits

Corresponding author: Bachir Taouli, MD, Department of Radiology and Translational and Molecular Imaging Institute, Icahn School of Medicine at Mount Sinai, 1470 Madison Avenue, New York, NY 10029, Tel: (212) 824-8453, bachir.taouli@mountsinai.org.

of agreement ([−75%,75%]). Test-retest repeatability was excellent in large vessels (CV=1–15%, bias=1–25%, BALA=[4%,150%]), and poor in small vessels (CV=7–130%, bias=10–200%, BALA=[8%,190%]). Average velocity in the right hepatic vein and average area of the splenic vein were higher in cirrhosis (p=0.027/0.0039). Flow in the middle hepatic vein strongly correlated with Child-Pugh score (ρ=0.84, p=0.0238), while flow in the splenic vein (ρ=0.43,p=0.032), time-average (ρ=0.46,p=0.02) and peak velocity in the superior mesenteric vein (ρ=0.45,p=0.032), and peak velocity in the infrarenal IVC (ρ=0.39,p=0.032) positively correlated to an imaging-based portal hypertension score. Average area of the splenic vein predicted cirrhosis [p=0.019; AUC(95% CI)=0.87(0.71,1.00)] and clinically significant portal hypertension [p=0.042; AUC(95% CI)=0.78(0.57–0.99)].

DATA CONCLUSION: Spiral 4D flow allows comprehensive assessment of abdominal vessels in one breath-hold, with substantial interobserver reproducibility, but variable test-retest repeatability. 4D flow may potentially reflect vascular changes due to cirrhosis and portal hypertension.

Keywords

4D flow; phase contrast MRI; spiral; liver fibrosis; cirrhosis; portal hypertension

Introduction

Portal hypertension (PH) is commonly present in patients with cirrhosis and can lead to high morbidity and mortality[1]. The hepatic venous pressure gradient (HVPG), which is the transvenous measurement of the pressure difference between the portal vein and the inferior vena cava (IVC) is an accepted indirect measurement of portal pressure for diagnosing and assessing the severity of PH[1,2]. HVPG has been shown to provide prognostic information and predict the development of complications of PH including bleeding from gastroesophageal varices[3,4]. However, HVPG measurement is relatively invasive, costly, and not available at all institutions[5]. These limitations underlie the need for non-invasive methods of assessing PH.

Doppler ultrasound (US) has been used to assess the severity of PH and changes in portal and splanchnic blood flow in liver disease, with variable results[6–12]. In addition, Doppler US has limited inter-observer reproducibility[13–16]. Two-dimensional phase-contrast MRI (2D PCMRI) directly evaluates blood flow dynamics and has been shown to be an effective noninvasive and reproducible technique for the assessment of PH[2,17–19]. However, 2D PC-MRI requires the use of double-oblique imaging planes, which is difficult and time consuming to position in coordination with patient breath-holds[20]. Additionally, this technique only allows visualization of large splanchnic vessels such as the portal vein (PV), which may be insufficient for a comprehensive flow evaluation[2].

4D flow MRI mapping using PC pulse sequences with 3D vascular coverage and 3-direction velocity encoding is a promising technique for comprehensive hemodynamic analysis by providing both co-registered anatomic and hemodynamic information 21–25. 4D flow Cartesian sequences with cardiac and respiratory triggering have acquisition times on the order of 10–20 minutes[23]. 4D flow MRI has been validated against 2D PC-MRI and Doppler US for measurement of blood flow in recent studies[20,23–26]. A non-Cartesian sampling

combined with compressed sensing allowing the acquisition of 4D flow data covering the major abdominal vessels in a single breath-hold has been recently described[25]. Previously published work on non-Cartesian 4D flow sequences showed strong interobserver agreement in image quality scores[25], and in quantitative flow parameters for the portal vein and hepatic artery[20,27], but did not report test-retest repeatability results.

Hence, the objectives of this study were to: 1) Determine the reproducibility and repeatability of flow quantification parameters in abdominal vessels using a breath-hold 4D flow spiral PC-MRI sequence combined with compressed sensing; 2) Assess the value of 4D flow parameters for predicting the presence of cirrhosis/PH and the severity of liver disease.

Materials and Methods

Patients

This prospective, single-center study complied with the Health Insurance Portability and Accountability Act. The study was approved by the local IRB and written informed consent was obtained from all subjects. Between March 2015 and March 2017, 54 patients with chronic liver disease underwent abdominal MRI with cardiac-triggered, phase-contrast MRI evaluation (Fig. 1). Patients with clinically indicated abdominal MRI for chronic liver disease follow-up and hepatocellular carcinoma screening/surveillance were included.

Clinical data

Age, sex, histopathologic liver fibrosis stage (when available), the presence of gastroesophageal varices on upper gastrointestinal endoscopy (when available), and portal hypertension composite imaging score[5] were recorded and calculated for all patients at the time of the MRI exam. In patients who had clinical histopathological evaluation of liver biopsy samples (n=25; time interval between MRI and biopsy, 485±780 days, range 7–2510 days), METAVIR (in chronic HBV/HCV) or the Brunt (in NASH) semiquantitative scoring systems[28,29] were used for histopathologic determination of the stage of fibrosis (fibrosis stage: F0-F4). In patients without liver biopsy, cirrhosis was diagnosed from clinical history (n=1 pre liver transplant patient), morphologic MRI findings (n=4; liver surface nodularity and findings of PH), or liver stiffness measurements by magnetic resonance elastography (MRE; n=7 patients) according to published liver stiffness cut-off values of cirrhosis[30,31]. The Child-Pugh and the Model of End-Stage Liver Disease (MELD) scores were calculated in cirrhotic patients[28–30]. For all patients, a non-invasive, imaging-based PH composite score (Table 1) was calculated, previously validated against HVPG measurement[5]. The PH composite score rates the presence and severity of abdominal ascites, the maximum cranio-caudal diameter of the spleen, and the number of variceal sites on a scale of 0 to 3, each. The PH composite score was determined from qualitative evaluation of the MRI exam by a radiologist with 1 year of abdominal MRI experience (S.P.).

Image acquisition

All patients were instructed to fast for at least 2–4 hours before the MRI exam. Patients were imaged on a 1.5T system (Magnetom Aera, Siemens Healthineers, Erlangen, Germany) equipped with a 30-channel spine and flexible body array coil for RF receiving and 33

mT/m maximum gradient strength. All patients were imaged with a cardiac-triggered, PC sequence with 3D velocity encoding (velocity encoding parameter VENC=60 cm/sec in each direction) and undersampled variable-density spiral trajectory ("spiral 4D flow")[25] acquired before injection of gadobenate dimeglumine (MultiHance, Bracco Diagnostics Inc., Monroe Township, NJ; n=21) or 10 min after injection of gadoxetic acid (Primovist/Eovist, Bayer Healthcare, Whippany, NJ; n=31). A coronal-oblique abdominal 60 mm slab (TR/TE/FA 16.5/3.8/9, FOV 400×400 mm, acquired matrix size 160 × 160 × 12, acquired voxel size 2.5 × 2.5 × 5 mm^3, interpolated voxel size 1.3 × 1.3 × 2.5 mm^3, temporal resolution 66–71 ms, acceleration factor of 6), covering abdominal vessels, was acquired over 24 cardiac cycles, in one 22-sec breath-hold at end expiration[25]. Four patients underwent repeat (test-retest) imaging, in two separate breath-holds within the same MRI exam, without moving or repositioning the patients.

In addition to the spiral 4D flow acquisition, the MRI protocol also included the following standard sequences: axial and coronal single-shot T_2-weighted imaging; axial fat-suppressed fast spin echo T_2-weighted imaging; axial 3D T_1-weighted imaging in- and out-of-phase, axial diffusion-weighted imaging; and 3D T_1-VIBE before and after injection of a gadolinium-based contrast agent (at approximately 4 min in n= 21 patients who had dynamic contrast-enhanced MRI acquisitions 8 sec before, during and up to 4 min. post injection of gadobenate dimeglumine; at 20 sec, 1 min, 10 and 20 minutes after injection of gadoxetic acid).

Image analysis

Image reconstruction was performed offline using a dynamic compressed sensing framework and an open-source GPU re-gridding software for radial 3D MRI, implemented in MATLAB R2016a (The MathWorks, Natick, MA)[25,32]. Reconstruction of each dataset took approximately 1 hour with use of a computing server (32 Intel Xeon CPUs, 2.2GHz, 256 GB RAM, K20 NVIDIA graphics card) running the Linux Ubuntu operating system. Images were analyzed using prototype software (Siemens Healthineers, Princeton, NJ) for 4D flow data visualization and vessel segmentation using a centerline model[33]. After performing corrections for phase aliasing, eddy currents and motion, up to 13 hepatic vessels, including the aorta and its celiac branches, the portal vein (PV) and inferior vena cava (IVC) (Fig. 2), were identified and segmented[25] by two observers in consensus (O.B., an MRI physicist with 4 years of experience, and M.W., a body MRI radiologist with 6 years of experience). Anatomical T_2-weighted and post-contrast T_1-weighted imaging was used as a reference to identify the abdominal vessels. A third independent observer (S.P., a body MRI fellow with 1 year of experience) performed vessel segmentation for a subsample of 15 cases for the purpose of inter-observer reproducibility assessment. Time-averaged vessel cross-section area, peak and time-averaged through-plane velocity, and net flow were measured.

Statistical analysis

Statistical analysis was performed using MATLAB, SPSS (version 20.0; IBM SPSS Inc, Armonk, NY) and GraphPad Prism 5.0 software (GraphPad Software, Inc., San Diego, CA). Inter-observer reproducibility and test-retest repeatability of vessel identification was evaluated by Cohen's kappa. Kappa values < 0.2 represent poor agreement, 0.21–0.40, fair

agreement, 0.41–0.60, moderate agreement, 0.61–0.80, substantial agreement, and 0.81–1.00 excellent agreement[34]. Interobserver and test-retest agreement of area, velocity and flow measurements were evaluated by coefficient of variation (CV) and Bland-Altman statistics. Flow parameters in all vessels were compared between patients grouped according to cirrhosis status, PH, MELD and Child-Pugh scores, using Mann-Whitney tests. Flow parameters were correlated to MELD and Child-Pugh scores by Spearman correlation. The diagnostic utility of hemodynamic parameters that showed significant differences between groups or trends towards significance was tested using binary logistic regression and ROC analysis. A stepwise model selection procedure based on the Wald statistic was used to select the best combination of hemodynamic and clinical covariates (age, gender, HCV/HBV status, alcohol abuse) for the prediction of cirrhosis, PH and clinically significant PH. Two-tailed p-values <0.05 were considered to be statistically significant; p-values between 0.05 and 0.1 were considered to show a trend towards statistical significance.

Results

Clinical data

The final population included 52 patients (Fig. 1; M/F 32/20, mean age 57 y, age range 22–82 y); two patients were excluded because of poor image quality on PC-MRI (Table 1). Cirrhosis was diagnosed in 48% of patients (n=25) based on biopsy (n=10) or liver stiffness measured with MRE (threshold for cirrhosis: >5 kPa) (n=10)[30] or morphologic changes on MRI (n=5). Based on the PH composite score cut-off (≥3) indicating PH (HVPG ≥ 5 mmHg), 26 of 52 patients were suspected of PH or clinically significant PH. PH scores shown to correspond with clinically significant PH (HVPG ≥ 10 mmHg, PH composite score ≥4) were observed in 21 patients (40% of patients).

Inter-observer reproducibility

In 15 patients, both observers identified 136 (70%) out of 195 abdominal vessels (up to 13 vessels per patient). Tables 2 and 3 show interobserver statistics for individual vessels, and all vessels combined. There was substantial overall agreement between observers in segmenting the vessels (all vessels Cohen's kappa=0.70, p<0.001). The celiac trunk and the supraceliac aorta were segmented with perfect inter-observer agreement (kappa=1, p=0.002), while the superior mesenteric artery (SMA) had the poorest interobserver agreement (kappa=0.42, p=0.101). For all vessels combined, area, velocity and flow measurements showed acceptable agreement between observers, with CV <21%, Bland-Altman bias <5%, but with high limits of agreement ([−75%, 75%]). Area measurements in the infrarenal aorta had the best inter-observer reproducibility (Table 2). The best inter-observer agreement for average velocity and flow was observed in the splenic vein, whereas the PV had the best interobserver agreement for peak velocity (Table 3).

Test-retest repeatability

Test-retest statistics for all vessels and individual vessels in 4 patients are presented in Tables 4 and 5. For all vessels combined, area, velocity and flow measurements showed modest test-retest agreement, with Cohen's kappa=0.50, CV <40%, Bland-Altman bias <55%, and high limits of agreement ([−150%, 150%]). The supraceliac aorta, hepatic, celiac and splenic

arteries, were identified with perfect agreement between test and re-test acquisitions (Cohen's kappa=1, p<0.001). The PV, splenic vein and SMV were identified with substantial agreement (Cohen's kappa >0.7, p< 0.001). The best test-retest agreement was observed in the PV for average velocity (CV=3.2%, bias=−4.5%) and maximum velocity (CV=5.2%, bias=−7.4%), in the SMV for area measurements (CV=1%, bias=1.4%), and in the infrarenal IVC for flow (CV=11.1%, bias= 15.7%). The poorest agreement in hemodynamic parameters was observed for the splenic artery (CV=16–140%, bias=23–200%) and SMA (CV=20–60%, bias=30–100%, BALA=[8%,188.7%]). Because these vessels were identified in test and retest sessions in only 1 patient, BALA are not available.

Prediction of cirrhosis and severity of cirrhosis

Compared to patients without cirrhosis, patients with cirrhosis had significantly increased mean area of the splenic vein (Fig.3a; p=0.0039) and increased mean velocity in the right hepatic vein (Fig.3b; p=0.027). No significant differences in the flow parameters measured in other vessels were observed between these groups of patients. The model selection procedure identified splenic vein area as a significant predictor of cirrhosis [p=0.019; AUC (95% CI) =0.87 (0.71,1.00)].

Correlation with MELD and Child-Pugh scores

Among patients with cirrhosis, we observed trends of negative correlations between the MELD score and flow (Spearman's ρ=−0.5, p=0.06) and peak velocity (ρ=−0.48, p=0.087) of the PV, and area (ρ=−0.76, p=0.06) of the SMV. Peak velocity in the splenic artery was negatively correlated with Child-Pugh score (ρ=−0.52, p=0.0493; Fig. 4a). Flow in the middle hepatic vein was strongly positively correlated with Child-Pugh score (ρ=0.84, p=0.0238; Fig. 4a). There were also trends of negative correlation of peak velocity in the suprarenal IVC (ρ=−0.46, p=0.06), and positive correlation of area (ρ=0.73, p=0.08) in the middle hepatic vein with the Child-Pugh score. Cross-sectional area of the PV was significantly decreased (p=0.035) in patients with Child-Pugh B (Fig. 5a) compared with patients with Child-Pugh A class. For patients with Child-Pugh's B and C, there was a trend of decreased PV cross-sectional area (p=0.097) and flow (p=0.097) compared to patients with Child-Pugh A. No significant correlations were observed between MELD and Child-Pugh scores and flow parameters in other vessels.

Prediction of PH and severity of PH

We observed significant weak to moderate positive correlations between PH score and flow in the splenic vein (ρ=0.43, p=0.032), average (ρ=0.46, p=0.02), and peak velocity in the SMV (ρ=0.45, p=0.032), and peak velocity in the infrarenal IVC (ρ=0.39, p=0.032) (Fig. 4b). For patients with imaging-based PH composite score ≥ 3 (Fig. 5b), corresponding to PH, infrarenal IVC area was significantly decreased (p=0.047). For patients with PH composite score ≥ 4 (Fig. 5c), corresponding to clinically significant PH, average velocity was increased in the supraceliac aorta (p=0.017). Trends of decreased peak velocities in the SMA (p=0.05) and supraceliac aorta (p=0.05) were observed for patients with PH or clinically significant PH. There was a trend of increased area in the splenic vein (p=0.057) in patients with clinically significant PH. There were no significant predictors for PH, while for clinically significant PH, SV area was a significant predictor [p=0.042; AUC (95%

CI)=0.78(0.57–0.99)]. A binary logistic regression model with SV area (p=0.046) and alcohol abuse (p=0.99) as covariates was identified by the model selection procedure as the best predictor of clinically significant PH [AUC (95% CI)=0.96 (0.88–1.00)].

Discussion

4D flow MRI has emerged as a valuable non-invasive technique for evaluation of hepatic and splanchnic hemodynamics[20,21,23–25,27,35,36]. Initial human studies showed feasibility in small cohorts, with focus on hepatic vessel visualization[37], and subsequently on quantification of hepatic flow parameters with Cartesian[21,23,24] and non-Cartesian 4D flow MRI[20,25], and comparison of flow parameters with Doppler US[24], 2D PC-MRI[25], and between the Cartesian and spiral techniques[25]. More recent studies used radial 4D flow to monitor hepatic and splanchnic flow in a porcine model of acute pre-hepatic PH[36], in healthy volunteers and patients with PH undergoing a meal challenge[27], and in PH patients before and after transjugular intrahepatic portosystemic shunt (TIPS) placement[35]. The present study expands the scope of previous studies by assessing interobserver agreement of vessel identification and quantitative parameters in hepatic and splanchnic vessels, test-retest repeatability, and correlation of 4D flow parameters with clinical parameters in a larger series of patients with chronic liver disease.

Blood flow measurements in abdominal vessels with a single-breath hold, spiral 4D flow MRI sequence is feasible, with comparable interobserver reproducibility to a previous study of the portal circulation using a Cartesian 4D flow respiratory gated acquisition with 20 min. acquisition time[21]. We also observed substantial to excellent test-retest agreement for identifying the hepatic and celiac arteries, portal vein, splenic and superior mesenteric vein, but variable agreement for quantitative parameters (depending on the vessels). The repeatability results are possibly influenced by the small number of patients (n=4), as well as by the limited resolution and coverage of the acquisition, combined with changes in vessel positions during breath-holds at end-expiration. Moreover, the same vessels were not always identified on the two test-retest acquisitions, which makes repeatability measures such as coefficient of variation and Bland-Altman statistics less robust.

In our patient cohort, increased area in the splenic vein was a significant predictor of cirrhosis. Increased splenic vein area and flow were observed by other investigators in patients with cirrhosis vs. age-matched controls[23]. These differences in hemodynamic parameters may be due to changes in vascular geometry and hyperdynamic circulation in cirrhosis[23], or splenomegaly and splenorenal shunting in cirrhosis and PH. Area of the splenic vein predicted PH scores corresponding to clinically significant PH, with increased AUC when combined with alcoholic etiology of liver disease. Although only 5 patients in our cohort (10%) had alcoholic liver disease, and their charts reported abstinence from alcohol for 2 years or more up to the time of MRI, 4 out of the 5 had Child-Pugh B cirrhosis, and they all had PH scores ≥ 4. Although the high combination AUC may be particular to our patient cohort, previous studies have shown alcohol consumption in alcoholic liver disease to increase HVPG and worsen complications of PH[38]. Increased average velocity and flow in the right hepatic vein were also observed in cirrhotic patients. While previous PC-MRI studies in liver disease did not perform measurements in the hepatic veins, previous

studies of cirrhosis and PH with Doppler ultrasound show a shift in the waveform pattern in the right or middle hepatic vein, from triphasic to monophasic, with increased severity of cirrhosis and PH[6,7,9–11].

Previous smaller studies (n=5–21 patients) found no statistical correlation of flow parameters with MELD or Child-Pugh scores in patients with cirrhosis[23,24]. We observed borderline significant, negative correlations with MELD score for flow and peak velocity in the PV, and of area in the SMV. Cross-sectional area of the PV was also significantly decreased in patients with Child-Pugh Class B compared with patients with Child-Pugh Class A, and there was a trend of decreasing area and flow for Child-Pugh Class B or C patients, findings also observed in a smaller 4D flow study in 20 cirrhotic patients[23]. The trend of decreasing portal flow with severity of cirrhosis is consistent with a large 2D phase-contrast MRI study (n=69), which found decreasing portal flow in patients with Child-Pugh's B compared to patients with Child-Pugh's A, but without statistical significance[2]. The decrease in PV area with cirrhosis severity is unexpected, considering Doppler flow studies that have shown portal diameter may exceed 13 mm in patients with cirrhosis and portal hypertension[7]. The discrepancy between Doppler and 4D flow PV area measurements can be explained by vessel diameter variation during respiratory phases/ breath-holds and different measurement locations in the PV. Decrease in the PV area has been documented in cirrhosis due to hepatic arterial buffer response (e.g. narrow PV, enlarged hepatic artery), and bi-phasic or hepatofugal flow[8].

The positive correlation of flow in the middle hepatic vein, as well as the trends of positive correlation for the area in middle hepatic vein and negative correlation for peak velocity in the suprarenal IVC, with Child-Pugh score were not observed in previous 4D flow studies. Regional flow acceleration has been previously observed on Doppler ultrasound of the middle and right hepatic veins in patients with cirrhosis because of compression by regenerative nodules and dampening of the pulsatile flow[8].The negative correlation between Child-Pugh score and peak velocity in the splenic artery contradicts previous Doppler studies that showed increase or no change in the splenic artery resistive index calculated based on peak systolic velocity in cirrhosis[6,8]. This finding may be due to the high variability of measurements in the splenic artery, as shown by limited interobserver and test-retest statistics.

The examination of 4D flow parameters in relation to PH revealed moderate positive correlations to flow in the splenic vein, average and peak velocity in the SMV, and peak velocity in the infrarenal IVC (in concordance with decrease in area of the infrarenal IVC in patients with PH and clinically significant PH). Increased splenic vein velocity and flow measurements in cirrhotic patients predicted esophageal varices in a previous Doppler study[6], while 4D flow measurements of SMV velocity and flow increased with severity of cirrhosis[23]. Increased time-averaged velocity was also observed in the supraceliac aorta for patients with clinically significant PH, which is consistent with hyperdynamic circulation in patients with PH[12,20].

Our study has several limitations. Cirrhosis status was determined from MRI and MRE findings, in the absence of liver histopathology in half of patients. The previously validated,

imaging-based PH composite score[5] was used as a surrogate for the invasive HVPG measurement. In terms of technical limitations, the breath-hold acquisition resulted in moderate anterior-posterior spatial coverage and moderate spatial resolution, which is not ideal to identify and measure flow in the hepatic arterial tree, or portal circulation collaterals. The spatial resolution and coverage can be improved by using concatenated breath-holds, or higher acceleration factor. While the spiral acquisition with compressed sensing considerably reduces acquisition time, post-processing for the 4D flow datasets requires 30 minutes - 1 hour of experienced user interaction. Furthermore, the semi-automatic, vessel centerline segmentation used in this work is subjective, and may result in poorer identification of some vessels.

Future work will include improvements to the 4D flow acquisition and post-processing, and will correlate flow data with degree of PH based on direct HVPG measurement. Qualitative assessment of 3D flow streamline patterns[20,23], as well as other hemodynamic metrics, such as flow[39] and pulsatility indices[7], pulse wave velocities and flow-derived pressure gradients in the portal and splanchnic veins and hepatic/splenic arteries will be investigated. Correlating 4D flow with magnetic resonance elastography (MRE) measurements of liver and spleen stiffness and invasive HVPG measurements would allow separation of the static component (reflecting the intrinsic mechanical properties of liver/spleen tissue) from the dynamic component (reflecting hemodynamic effects from PH) of liver and spleen shear stiffness. 4D flow measurements will be included in larger studies aiming to validate multiparametric MRI predictive models combining tissue viscoelastic properties and splanchnic flow parameters as non-invasive biomarkers of portal hypertension and severity of portal hypertension. The development of such predictive models may have major impact on prognosis, for establishing the risk of hepatic decompensation and bleeding.

In conclusion, a spiral 4D flow sequence allows comprehensive assessment of abdominal vessel flow parameters in a single breath-hold. Hemodynamic parameters in the splanchnic vessels were measured with substantial interobserver reproducibility and variable test-retest repeatability, and may potentially reflect vascular changes due to cirrhosis and PH.

Acknowledgement

This study was supported by funding from the NIH NIDDK grants 1R01DK08787, 1F32DK109591 (fellowship,O.B.), and Société Française de Radiologie (fellowship, M.W.).

ABBREVIATIONS (in alphabetic order)

BALA	Bland-Altman limits of agreement
CV	coefficient of variation
HVPG	hepatic venous pressure gradient
IVC	inferior vena cava
MELD	Model of End-Stage Liver Disease
MRI	magnetic resonance imaging

PC	phase-contrast
PH	portal hypertension
PV	portal vein
SMA	superior mesenteric artery
SMV	superior mesenteric vein
VENC	velocity encoding parameter

References

1. Haj M, Rockey DC. Predictors of clinical outcomes in cirrhosis patients. Current Opinion in Gastroenterololgy 2018;34(4)(1531–7056 (Electronic)):266–271.
2. Gouya H, Grabar S, Vignaux O, et al. Portal hypertension in patients with cirrhosis: indirect assessment of hepatic venous pressure gradient by measuring azygos flow with 2D-cine phase-contrast magnetic resonance imaging. European radiology 2016;26(7):1981–1990. [PubMed: 26373753]
3. Groszmann RJ, Garcia-Tsao G, Bosch J, et al. Beta-blockers to prevent gastroesophageal varices in patients with cirrhosis. The New England journal of medicine 2005;353(21):2254–2261. [PubMed: 16306522]
4. Groszmann RJ, Wongcharatrawee S. The hepatic venous pressure gradient: anything worth doing should be done right. Hepatology (Baltimore, Md) 2004;39(2):280–282.
5. Kihira S, Kagen AC, Vasudevan P, et al. Non-invasive prediction of portal pressures using CT and MRI in chronic liver disease. Abdominal radiology (New York) 2016;41(1):42–49. [PubMed: 26830610]
6. Baik SK. Haemodynamic evaluation by Doppler ultrasonography in patients with portal hypertension: a review. Liver international : official journal of the International Association for the Study of the Liver 2010;30(10):1403–1413. [PubMed: 20731772]
7. Baik SK, Kim JW, Kim HS, et al. Recent Variceal Bleeding: Doppler US Hepatic Vein Waveform in Assessment of Severity of Portal Hypertension and Vasoactive Drug Response. Radiology 2006;240(2):574–580. [PubMed: 16864678]
8. Goyal N, Jain N, Rachapalli V, Cochlin DL, Robinson M. Non-invasive evaluation of liver cirrhosis using ultrasound. Clinical Radiology 2009;64(11):1056–1066. [PubMed: 19822238]
9. Iranpour P, Lall C, Houshyar R, et al. Altered Doppler flow patterns in cirrhosis patients: an overview. Ultrasonography (Seoul, Korea) 2016;35(1):3–12.
10. Kim MY, Baik SK, Park DH, et al. Damping index of Doppler hepatic vein waveform to assess the severity of portal hypertension and response to propranolol in liver cirrhosis: a prospective nonrandomized study. Liver international : official journal of the International Association for the Study of the Liver 2007;27(8):1103–1110. [PubMed: 17845539]
11. Zardi EM, Di Matteo FM, Pacella CM, Sanyal AJ. Invasive and non-invasive techniques for detecting portal hypertension and predicting variceal bleeding in cirrhosis: A review. Annals of Medicine 2014;46(1):8–17. [PubMed: 24328372]
12. Moller S, Hobolth L, Winkler C, Bendtsen F, Christensen E. Determinants of the hyperdynamic circulation and central hypovolaemia in cirrhosis. Gut 2011;60(9):1254–1259. [PubMed: 21504996]
13. Palaniyappan N, Cox E, Bradley C, et al. Non-invasive assessment of portal hypertension using quantitative magnetic resonance imaging. Journal of hepatology 2016;65(6):1131–1139. [PubMed: 27475617]
14. Sacerdoti D, Gaiani S, Buonamico P, et al. Interobserver and interequipment variability of hepatic, splenic, and renal arterial Doppler resistance indices in normal subjects and patients with cirrhosis. Journal of hepatology 1997;27(6):986–992. [PubMed: 9453423]

15. Sabba C, Weltin GG, Cicchetti DV, et al. Observer variability in echo-Doppler measurements of portal flow in cirrhotic patients and normal volunteers. Gastroenterology 1990;98(6):1603–1611. [PubMed: 2186953]
16. Paulson EK, Kliewer MA, Frederick MG, Keogan MT, DeLong DM, Nelson RC. Doppler US measurement of portal venous flow: variability in healthy fasting volunteers. Radiology 1997;202(3):721–724. [PubMed: 9051024]
17. Burkart DJ, Johnson CD, Ehman RL, Weaver AL, Ilstrup DM. Evaluation of portal venous hypertension with cine phase-contrast MR flow measurements: high association of hyperdynamic portal flow with variceal hemorrhage. Radiology 1993;188(3):643–648. [PubMed: 8351326]
18. Gouya H, Vignaux O, Sogni P, et al. Chronic liver disease: systemic and splanchnic venous flow mapping with optimized cine phase-contrast MR imaging validated in a phantom model and prospectively evaluated in patients. Radiology 2011;261(1):144–155. [PubMed: 21771955]
19. Wu MT, Pan HB, Chen C, et al. Azygos blood flow in cirrhosis: measurement with MR imaging and correlation with variceal hemorrhage. Radiology 1996;198(2):457–462. [PubMed: 8596849]
20. Roldan-Alzate A, Frydrychowicz A, Niespodzany E, et al. In vivo validation of 4D flow MRI for assessing the hemodynamics of portal hypertension. Journal of magnetic resonance imaging : JMRI 2013;37(5):1100–1108. [PubMed: 23148034]
21. Stankovic Z, Frydrychowicz A, Csatari Z, et al. MR-based visualization and quantification of three-dimensional flow characteristics in the portal venous system. Journal of magnetic resonance imaging : JMRI 2010;32(2):466–475. [PubMed: 20677279]
22. Frydrychowicz A, Francois CJ, Turski PA. Four-dimensional phase contrast magnetic resonance angiography: potential clinical applications. European journal of radiology 2011;80(1):24–35. [PubMed: 21333479]
23. Stankovic Z, Csatari Z, Deibert P, et al. Normal and altered three-dimensional portal venous hemodynamics in patients with liver cirrhosis. Radiology 2012;262(3):862–873. [PubMed: 22357888]
24. Stankovic Z, Csatari Z, Deibert P, et al. A feasibility study to evaluate splanchnic arterial and venous hemodynamics by flow-sensitive 4D MRI compared with Doppler ultrasound in patients with cirrhosis and controls. European journal of gastroenterology & hepatology 2013;25(6):669–675. [PubMed: 23411868]
25. Dyvorne H, Knight-Greenfield A, Jajamovich G, et al. Abdominal 4D flow MR imaging in a breath hold: combination of spiral sampling and dynamic compressed sensing for highly accelerated acquisition. Radiology 2015;275(1):245–254. [PubMed: 25325326]
26. Yzet T, Bouzerar R, Allart JD, et al. Hepatic vascular flow measurements by phase contrast MRI and doppler echography: a comparative and reproducibility study. Journal of magnetic resonance imaging : JMRI 2010;31(3):579–588. [PubMed: 20187200]
27. Roldan-Alzate A, Frydrychowicz A, Said A, et al. Impaired regulation of portal venous flow in response to a meal challenge as quantified by 4D flow MRI. Journal of magnetic resonance imaging : JMRI 2015;42(4):1009–1017. [PubMed: 25772828]
28. Bedossa P, Poynard T. An algorithm for the grading of activity in chronic hepatitis C. The METAVIR Cooperative Study Group. Hepatology (Baltimore, Md) 1996;24(2):289–293.
29. Brunt EM, Janney CG, Bisceglie AMD, Neuschwander-Tetri BA, Bacon BR. Nonalcoholic steatohepatitis: a proposal for grading and staging the histological lesions. The American Journal of Gastroenterology 1999;94(9):2467–2474. [PubMed: 10484010]
30. Dyvorne HA, Jajamovich GH, Bane O, et al. Prospective comparison of magnetic resonance imaging to transient elastography and serum markers for liver fibrosis detection. Liver international : official journal of the International Association for the Study of the Liver 2016;36(5):659–666. [PubMed: 26744140]
31. Singh S, Venkatesh SK, Wang Z, et al. Diagnostic performance of magnetic resonance elastography in staging liver fibrosis: a systematic review and meta-analysis of individual participant data. Clinical gastroenterology and hepatology : the official clinical practice journal of the American Gastroenterological Association 2015;13(3):440–451 e446. [PubMed: 25305349]
32. Schwarzl A GPU Regridding of Radial 3D MRI Data. Graz, Austria: Graz University of Technology; 2012 36 p.

33. Gulsun MA, Jolly M-P, Guehring J, et al. A Novel 4D Flow Tool for Comprehensive Blood Flow Analysis In: ISMRM, Melbourne, Australia, 2012 (1176).

34. Landis JR, Koch GG. The measurement of observer agreement for categorical data. Biometrics 1977;33(1):159–174. [PubMed: 843571]

35. Bannas P, Roldan-Alzate A, Johnson KM, et al. Longitudinal Monitoring of Hepatic Blood Flow before and after TIPS by Using 4D-Flow MR Imaging. Radiology 2016;281(2):574–582. [PubMed: 27171019]

36. Frydrychowicz A, Roldan-Alzate A, Winslow E, et al. Comparison of radial 4D Flow-MRI with perivascular ultrasound to quantify blood flow in the abdomen and introduction of a porcine model of pre-hepatic portal hypertension. European radiology 2017.

37. Frydrychowicz A, Landgraf BR, Niespodzany E, et al. Four-dimensional velocity mapping of the hepatic and splanchnic vasculature with radial sampling at 3 tesla: a feasibility study in portal hypertension. Journal of magnetic resonance imaging : JMRI 2011;34(3):577–584. [PubMed: 21751287]

38. Restellini S, Goossens N, Clement S, et al. Collagen proportionate area correlates to hepatic venous pressure gradient in non-abstinent cirrhotic patients with alcoholic liver disease. World journal of hepatology 2018;10(1):73–81. [PubMed: 29399280]

39. Keller EJ, Kulik L, Stankovic Z, et al. JOURNAL CLUB: Four-Dimensional Flow MRI-Based Splenic Flow Index for Predicting Cirrhosis-Associated Hypersplenism. AJR American journal of roentgenology 2017;209(1):46–54. [PubMed: 28463524]

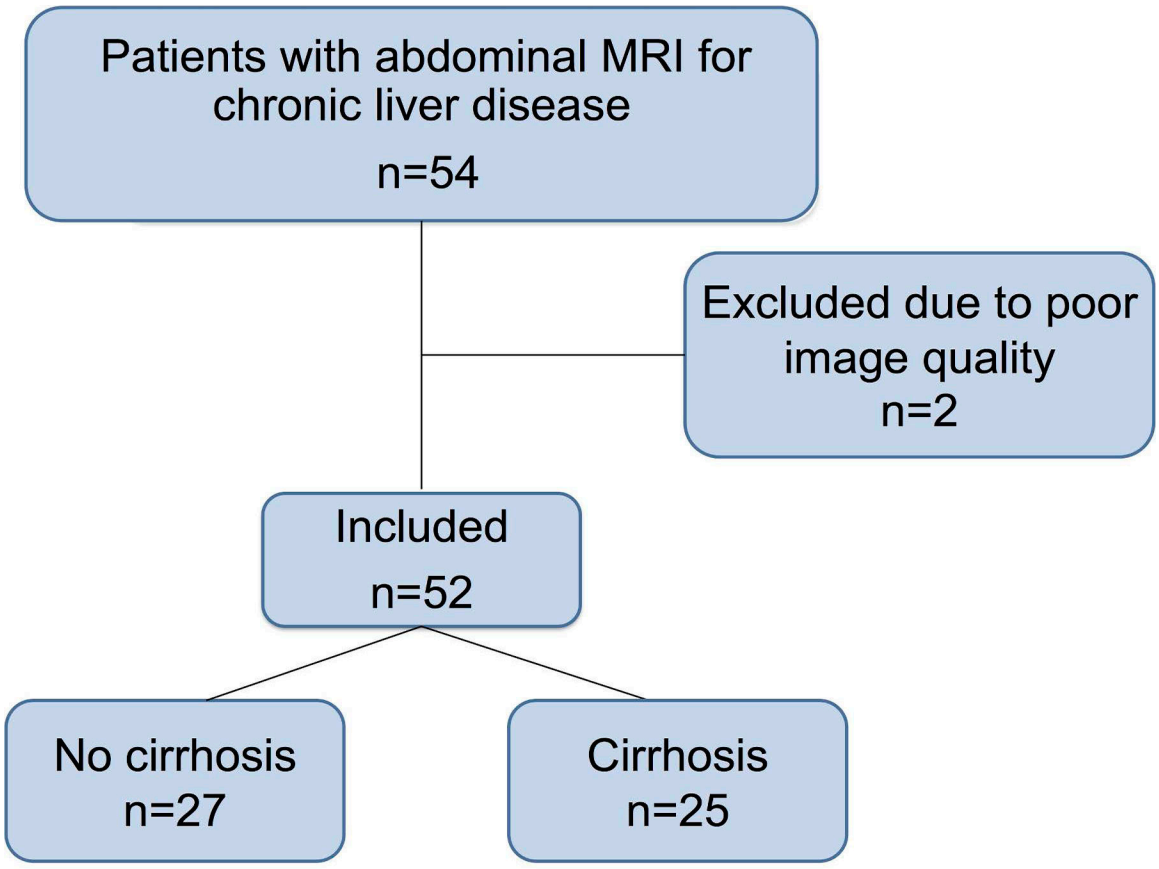

Fig.1.

Flow-chart showing selection of patients for 4D flow analysis. Patients with chronic liver disease referred for an abdominal MRI were selected for participation in the study.

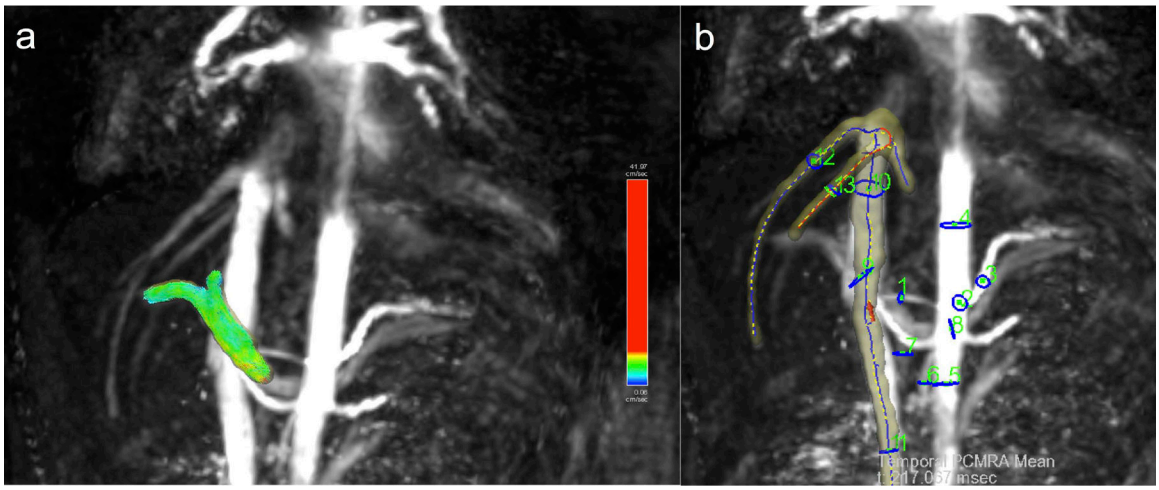

Fig.2.

Rendering of abdominal vessels in a patient (male, 22 years) with primary sclerosing cholangitis and advanced liver fibrosis (stage F3). a) Portal vein segmentation with particle tracing visualization; **b)** maximum intensity projection with 13 vessel segmentation and plane ROIs for flow measurements: hepatic artery (1), celiac trunk (2), splenic artery (3), supraceliac aorta (4), infrarenal aorta (5), superior mesenteric artery (6), superior mesenteric vein (7), splenic vein (8), portal vein (9), suprarenal IVC; 10), infrarenal IVC; right (12) and middle (13) hepatic veins.

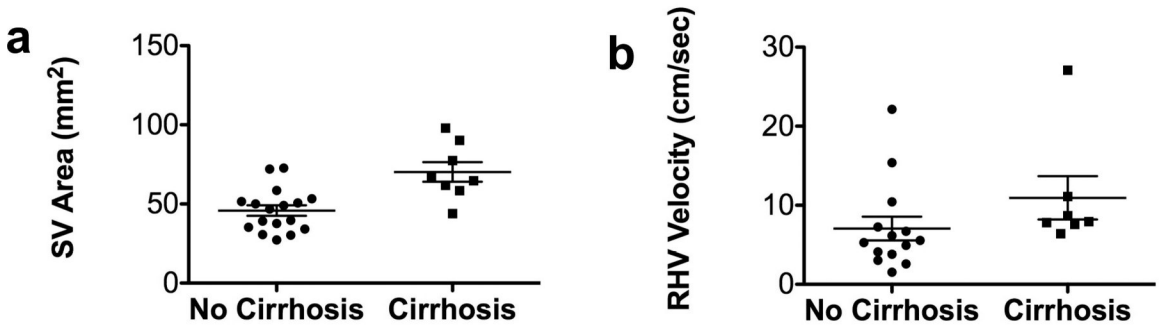

Fig.3.

Scatter plot distribution of 4D flow parameters (splenic vein area and right hepatic vein velocity) stratified by presence/absence of cirrhosis. The splenic vein (**a**) and right hepatic vein (**b**) showed significantly increased flow parameters in patients with cirrhosis. Mean cross-sectional area of the splenic vein in patients with cirrhosis (p=0.0039) and mean velocity in the right hepatic vein (p=0.027) were significantly increased in cirrhotic vs. noncirrhotic patients. Lines on data distribution plots correspond to mean ± standard error of the mean.

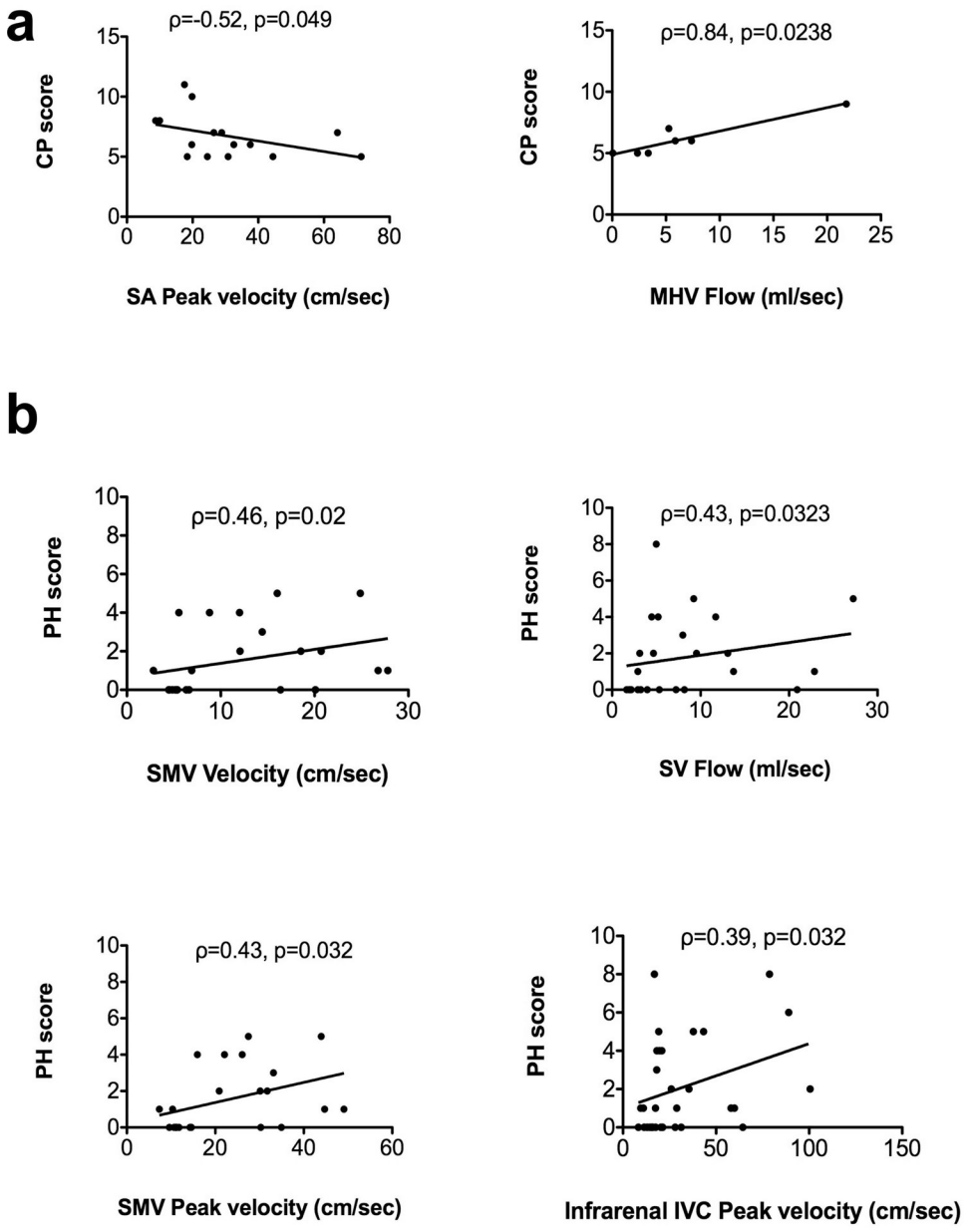

Fig.4.

Correlation plots of 4D flow parameters with severity of cirrhosis (**a**) and portal hypertension (**b**). Among patients with cirrhosis (**a**), peak velocity in the splenic artery (SA) was negatively correlated with Child-Pugh score, and flow in the middle hepatic vein (MHV) was positively correlated with Child-Pugh score. Among all patients (**b**), there were significant modest positive correlations between flow, velocity and peak velocity and portal hypertension (PH) score in the splenic vein (SV), SMV and infrarenal IVC, respectively.

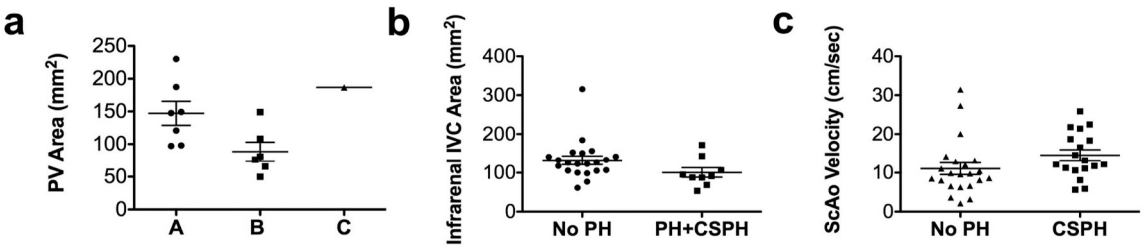

Fig.5.

Scatter plot distribution of 4D flow parameters stratified by severity of cirrhosis and portal hypertension. Cross-sectional area of the portal vein (PV) was significantly decreased in patients with Child-Pugh's class B compared to class A, but not to class C (**a**). For PH score ≥ 3, corresponding to PH or clinically significant portal hypertension, area was significantly decreased in the infrarenal inferior vena cava (IVC) (**b**; p=0.047). For PH score ≥ 4, corresponding to clinically significant portal hypertension, velocity was significantly increased in the supraceliac aorta (ScAo) (**c**; p=0.03). Lines on data distribution plots correspond to mean ± standard error of the mean.

Table 1:

Patient's characteristics.

	All patients (n=52)
Sex (M/F)	32/ 20
Age (mean ± SD) (y)	57±14
Etiology of chronic liver disease	
HCV*	27(52%)
HBV	6(11.5%)
NASH*	7(13.5%)
Alcohol abuse	5(10%)
Primary sclerosing cholangitis/auto-immune hepatitis*	4(7%)
Other**	3(6%)
Cirrhosis status	
No cirrhosis	27(52%)
Cirrhosis	25(48%)
PH composite score	
No portal hypertension (PH scores 0–2)	26(50%)
Portal hypertension (PH score=3)	5(10%)
Clinically significant portal hypertension (PH score >4)	21(40%)
MELD score (mean ± SD)	12 ± 5.4
Child-Pugh class	
A	13(25%)
B	9(17%)
C	3(6%)

Data are presented as mean ± standard deviation or number of cases (percentage of cases)

* includes 3 cases of HCV associated with another etiology, 2 cases with NASH associated with AIH, and 1 case of AIH associated with PSC,

** Non cirrhotic portal hypertension and nodular regenerative hyperplasia (n=1), hemochromatosis (n=1), cholangiocarcinoma with no underlying liver disease.

Table 2.

Inter-observer reproducibility metrics and identification for all 13 abdominal vessels (arteries and veins) and individual arteries measured in 15 patients.

		All vessels	Hepatic artery	Celiac trunk	Splenic artery	SMA	Supraceliac aorta	Infra renal aorta
	Cohen's kappa	**0.70**	**0.55**	**1.00**	**0.99**	**0.42**	**1.00**	**0.81**
	p	**<0.001**	**0.02**	**<0.001**	**<0.001**	**0.101**	**<0.001**	**0.001**
Area	CV (%)	14.9	25.6	15.9	11.8	18.8	11.2	5.6
	Bias (%)	−1.5	−2.4	−8.0	12.0	−4.2	6.2	−4.5
	BALA (%)	−58.8,55.8	−87.2,82.3	−61.0,45.0	−28.2,52.2	−72.7,64.2	−42.1,54.6	−25.5,16.5
Average Velocity	CV (%)	20.4	25.4	18.5	32.6	16.6	27.1	13.5
	Bias (%)	−10.5	−0.4	−6.2	−26.0	−4.3	−32.1	−4.2
	BALA (%)	−94.0, 73.0	−101.4,100.6	−71.4,59.0	−144.8,92.9	−79.9,71.3	−139.2,75.0	−54.5,46.1
Peak Velocity	CV (%)	17.5	23.2	32.0	31.2	14.8	12.2	7.7
	Bias (%)	−5.4	−4.7	−18.6	−11.5	−9.2	5.7	5.5
	BALA (%)	−73.12, 62.4	−91.5,82.1	−116.5,79.4	−113.4,90.3	−72.4,54.0	−49.4,60.9	−20.8,31.9
Flow	CV (%)	21.6	17.2	18.5	34.7	16.9	24.8	16.3
	Bias (%)	−11.3	−4.20	−14.1	−15.66	−8.58	−14.1	−6.64
	BALA (%)	−95.2,72.6	−70.8,62.4	−79.3,51.1	−142.4,111.1	−78.6,61.4	−113.6,85.4	−70.5,57.2

SMA=superior mesenteric artery; CV=coefficient of variation, BALA=Bland-Altman limits of agreement.

Table 3.

Inter-observer reproducibility metrics and identification for abdominal veins measured in 15 patients.

		PV	SMV	Splenic vein	Suprarenal IVC	Infrarenal IVC	Right Hepatic Vein	Middle Hepatic Vein
	Cohen's kappa	**0.63**	**0.48**	**0.67**	**0.63**	**0.70**	**0.86**	**0.60**
	p	**0.008**	**0.029**	**0.006**	**0.008**	**0.007**	**0.001**	**0.019**
Area	CV (%)	19.7	21.8	11.9	14.7	13.8	17.2	11.7
	Bias (%)	10.6	−7.0	−3.2	−7.1	−15.5	−8.4	−8.7
	BALA (%)	−70.6,91.8	−86.6,72.6	−47.3, 40.9	−59.9,45.7	−73.0,42.1	−75.0,58.2	−42.4,25.0
Average Velocity	CV (%)	13.2	22.4	10.6	14.1	16.8	25.7	40.8
	Bias (%)	−3.8	−6.8	12.1	11.2	−3.7	−26.8	−57.6
	BALA (%)	−56.4,48.8	−87.0,73.4	−26.0,50.2	−44.7,67.0	−64.2,56.8	−129.5,75.9	−161.2,45.9
Peak Velocity	CV (%)	10.1	13.6	13.8	14.0	14.7	14.7	32.6
	Bias (%)	2.1	−11.3	15.2	9.7	−11.4	−14.5	−46.1
	BALA (%)	−35.0,39.2	−62.6,40.0	−19.6,50.0	−40.7,60.1	−63.2,40.4	−94.3,65.2	−110.4,18.1
Flow	CV (%)	14.5	11.5	10.3	19.1	21.0	32.4	45.9
	Bias (%)	7.6	−14.6	8.9	4.3	−19.3	−35.1	−64.9
	BALA (%)	−48.6,63.8	−44.4,15.2	−25.3,43.1	−70.1,78.6	−94.3,55.7	−147.8,77.7	−166.8,37.0

Veins: IVC = inferior vena cava, PV=portal vein (intrahepatic), SMV=superior mesenteric vein, Data for the left hepatic vein was not analyzed, since this vessel could be segmented in only 6 out of 52 patients. CV=coefficient of variation, BALA=Bland-Altman limits of agreement.

Table 4.

Test-retest reproducibility metrics and identification for 13 vessels (arteries and veins) and individual arteries measured in 4 patients. SMA=superior mesenteric artery, CV=coefficient of variation, BALA=Bland-Altman limits of agreement. No BALA statistics are given for vessels with test-retest measurements in 1 patient.

		All vessels	Hepatic artery	Celiac trunk	Splenic artery	SMA	Supraceliac aorta	Infrarenal aorta
	Cohen's kappa	**0.50**	**1.00**	**1.00**	**1.00**	**0.87**	**1.00**	**0.87**
	p	**<0.001**	**<0.001**	**<0.001**	**<0.001**	**<0.001**	**<0.001**	**<0.001**
Area	CV (%)	15.4	6.8	14.3	16.4	20.3	15.5	10.2
	Bias (%)	−0.1	9.6	−13.9	23.1	28.7	−6.4	14.4
	BALA(%)	−56.4,56.3	−15.6,34.8	−67.0,39.2	-	12.1,45.3	−56.3,43.5	3.6,25.3
Average Velocity	CV (%)	35.8	18.1	17.9	135.6	51.3	30.4	51.0
	Bias (%)	−3.6	−24.0	−9.8	−191.7	72.5	29.9	33.8
	BALA(%)	−145.3,138.2	−90.3,42.4	−76.2,56.7	-	−34.6,179.6	−88.5,148.4	−174.5,242.1
Maximum Velocity	CV (%)	35.8	31.8	36.9	118.0	32.4	43.4	20.3
	Bias (%)	−14.6	2.9	−17.5	−166.9	45.9	−15.5	20.5
	BALA(%)	−136.1,106.9	−122.4,128.3	−137.7,102.7	-	45.7,46.1	−158.2,127.2	−57.7,98.8
Flow	CV (%)	38.7	22.6	16.0	134.0	69.8	29.5	53.8
	Bias (%)	−4.8	−14.3	−22.6	−189.5	98.8	23.5	43.4
	BALA(%)	−154.5,145.0	−101.9,73.3	−44.6,−0.6	-	8.8,188.7	−84.8,131.8	−164.6,251.4

Table 5.

Test-retest repeatability metrics and identification of abdominal veins measured in 4 patients.

		PV	SMV	Splenic vein	Suprarenal IVC	Infra renal IVC	Right Hepatic Vein	Middle Hepatic Vein
	Cohen's kappa	**0.74**	**0.74**	**0.73**	**0.87**	**0.74**	**0.87**	**0.87**
	p	**<0.001**	**<0.001**	**<0.001**	**<0.001**	**<0.001**	**<0.001**	**<0.001**
Area	CV (%)	9.9	1.0	-	32.4	19.0	-	31.5
	Bias (%)	−14.0	1.4	-	−45.8	−26.9	-	44.6
	BALA (%)	-	-	-	−145.2,53.7	-	-	-
Average Velocity	CV (%)	3.2	18.2	-	30.1	29.6	-	55.5
	Bias (%)	−4.5	−25.8	-	−42.5	41.8	-	−78.5
	BALA (%)	-	-	-	−86.6,1.6	-	-	-
Maximum Velocity	CV (%)	5.2	30.4	-	48.1	10.9	-	21.8
	Bias (%)	−7.4	−43.1	-	−68.1	15.4	-	−30.8
	BALA (%)	-	-	-	−174.3,38.1	-	-	-
Flow	CV (%)	13.0	17.2	-	57.1	11.1	-	26.7
	Bias (%)	−18.3	−24.4	-	−80.8	15.7	-	−37.7
	BALA (%)	-	-	-	−204.1,42.4	-	-	-

Vessels: IVC = inferior vena cava, PV=portal vein (intrahepatic), SMV=superior mesenteric vein. Data for the left hepatic vein was not analyzed, since this vessel could be segmented in only 6 out of 52 patients. CV=coefficient of variation, BALA=Bland-Altman limits of agreement.

No CV/ Bland-Altman bias for vessel which were not identified in test and re-test sessions. No BALA statistics for vessels with test-retest measurements in 1 patient.